A COMBINED LQR–BACKSTEPPING APPROACH FOR NONLINEAR BALL-AND-BEAM CONTROL

Hung-Tuan-Anh Tran [1], Trung-Hieu Le [2]*, Thi-Hong-Lam Le [1], Thi-Ngoc-Thao Nguyen [1], Thi-Ngoc-Hieu Phu [1], Hoang-Lam Le [1], Phong-Luu Nguyen [1], Thanh-Binh Nguyen [1]

[1] Ho Chi Minh City University of Technology and Engineering (HCM-UTE), Ho Chi Minh City (HCMC), Vietnam
Vo Van Ngan Str., No. 01, Thu Duc ward, HCMC, Vietnam

[2] Avery Dennison RBIS Long An Company
Suare E.01, Trung Tam Str., Can Giuoc ward, Tay Ninh province, Vietnam

* Corresponding author. E-mail: hieu.t.le@ap.averydennison.com

Abstract: This paper presents a hybrid LQR–Backstepping control approach for the ball-and-beam system, a nonlinear and inherently unstable system. The proposed method combines the optimal performance of LQR with the nonlinear stability of Backstepping to enhance both stabilization and trajectory tracking. Simulation results under fixed-point stabilization and sinusoidal tracking scenarios demonstrate fast response, low overshoot, and good tracking accuracy, confirming the effectiveness of the proposed approach for nonlinear control applications.
Keywords: Ball-and-beam system; LQR; Backstepping control; Hybrid control; Trajectory tracking.

1. Introduction

The ball-and-beam is a classical benchmark system in control engineering and is widely used to evaluate control strategies for nonlinear and underactuated systems. Due to its inherent instability and nonlinear dynamics, this system presents significant challenges in both stabilization and trajectory tracking tasks. In practical applications, the control objective is not only to keep the ball at a desired position but also to make the system follow time-varying reference trajectories while maintaining closed-loop stability. Similar control problems have been studied in pendulum-based systems, where optimal control techniques such as LQG have shown effectiveness in maintaining system stability under different operating conditions [1]. In addition, adaptive optimization approaches such as particle swarm optimization have been used to improve controller parameters [2]. Robust control strategies, including sliding mode control, have also been applied to handle uncertainties and disturbances in underactuated systems [3], [4].

Among various control methods, the Linear Quadratic Regulator (LQR) is widely used for its optimal state-feedback formulation. By minimizing a quadratic cost function, LQR balances tracking performance and control effort. LQR has been successfully applied to inverted pendulum systems and trajectory-tracking problems [7], [13]. Moreover, its performance can be improved by properly selecting or optimizing the weighting matrices, as reported in recent studies [10]. However, a major limitation of LQR is that it is typically designed using a linearized model around an operating point. Therefore, when the ball-and-beam system operates far from the equilibrium point or exhibits strong nonlinear behavior, the performance of a conventional LQR controller may degrade [9], [11].

PID control is another common approach due to its simple structure and ease of implementation. However, it does not explicitly account for the nonlinear dynamics of the ball-and-beam system. Its performance depends heavily on parameter tuning and may not provide a systematic stability guarantee for nonlinear underactuated systems. As a result, although PID control can be useful for simple regulation tasks, its application to nonlinear trajectory tracking may be limited.

To directly address nonlinear dynamics, Backstepping control has been developed as an effective nonlinear control design method. By recursively constructing Lyapunov functions, Backstepping can guarantee the stability of the closed-loop system and is suitable for underactuated systems such as the ball-and-beam system [5]. Nevertheless, pure Backstepping control may yield complex control laws. In addition, it does not inherently include an optimal feedback structure that balances tracking performance and control effort.

Recent research trends indicate that combining control strategies can improve overall control design. For example, adaptive and real-time trajectory-tracking methods with online parameter estimation have been proposed to enhance control performance in practical applications [6]. Furthermore, nonlinear and intelligent control approaches have been developed to address uncertainties and complex system dynamics [8], [12], [15]. These studies suggest that integrating nonlinear control with optimal control techniques is a promising direction for improving the control design of nonlinear systems.

Motivated by these considerations, this study proposes a combined LQR–Backstepping control strategy for the nonlinear ball-and-beam system. The main contribution of this work is the integration of the LQR gain structure into the Backstepping design framework. Unlike conventional LQR, which relies primarily on a linearized model, the proposed controller uses the LQR gain to define the tracking error surface within a nonlinear control design. Compared with pure Backstepping control, the proposed method provides a more structured feedback form by incorporating LQR gain information. Therefore, the proposed LQR–Backstepping controller is not simply a direct application of LQR or Backstepping, but a combined design that exploits both optimal state-feedback characteristics and Lyapunov-based nonlinear stability analysis.

The proposed controller is evaluated using two simulation cases, namely fixed-position stabilization and sinusoidal trajectory tracking. The results are analyzed to illustrate the behavior of the closed-loop system under the considered operating conditions. These cases demonstrate the feasibility of applying the proposed LQR–Backstepping design to the nonlinear ball-and-beam system.

2. Ball-and-Beam Model

Fig. 1 illustrates the mechanical structure and main components of the ball-and-beam system. The system consists of a beam of length L_{beam}, on which a ball moves with position r, while the beam angle is denoted by θ. The beam is actuated through a driving mechanism that includes an arm and a load gear, enabling adjustment of the beam angle to control the ball's position. This schematic clearly shows the interconnection between components and serves as the basis for dynamic modeling and controller design of the system.

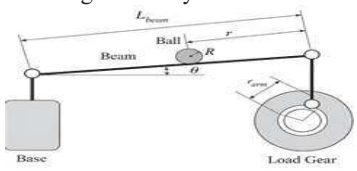


Fig. 1. Ball-and-beam model [16]

Tab. 1 System Parameters and Variables

Nr.	Symbol	Description	Value
1	$\alpha(t)$	Angular position of beam	*rad*
2	$r(t)$	Linear displacement of the ball along the beam	*m*
3	$\theta(t)$	Rotation angle of the motor-driven gear	*rad*
4	d	Radius of the driving disk	0.075 *m*
5	g	Acceleration due to gravity	9.81 *m/s²*
6	m	Mass of the ball	0.065 *kg*
7	M	Mass of the beam	0.34 *kg*
8	L	Total length of the beam	0.54 *m*
9	R	Radius of the ball	0.0125 *m*
10	u	Control input torque applied by the motor	*N·m*
11	J_B	Moment of inertia of ball	$\frac{2}{5}mR^2$
12	J_b	Moment of inertia of a beam	$\frac{1}{3}ML^2$
13	R_m	Motor resistance	6.83527(Ω)
14	K_t	Torque constant	0.064943 $(N.m/A)$
15	K_b	Back EMF constant	0.064943 $(V.s/rad)$
16	C_m	Coefficient of viscous friction	0.00034 $(N.m/(rad/s))$
17	J_m	Moment of Inertia of Rotor	0.000134 $(kg.m^2)$
18	L	Motor inductance	86.3H
19	K_x	Constant	$\frac{K_t}{R_m}$
20	K_y	Constant	$\frac{K_t.K_b}{R_m}$
21	K_z	Constant	$\frac{L.dt}{d}$
22	u	Voltage Input	(V)

Deriving the equations of motion for the ball and beam system first requires calculating the combined kinetic energy of both components. Using the Lagrangian method based on energy balance [17,18] and incorporating nonlinear equation methodologies from [19,20], our team developed the mathematical model describing the system's motion.

$$\frac{d\left(\frac{\partial \ell}{\partial \dot{q}_i}\right)}{dt} - \frac{\partial \ell}{\partial \dot{q}_i} = u_i (i = 1...n) \tag{1}$$

$$\frac{d\left(\frac{\partial \ell}{\partial \dot{\alpha}}\right)}{dt} - \frac{\partial \ell}{\partial} = \tau_b \tag{2}$$

$$\frac{d\left(\frac{\partial \ell}{\partial \dot{r}}\right)}{dt} - \frac{\partial \ell}{\partial \dot{r}} = 0 \tag{3}$$

By differentiating Equation (2) and (3), the differential equation of the system is given as follows:

$$\begin{bmatrix} \left(m_B r^2 + J_b\right)\ddot{\alpha} + 2m_B r\dot{r}\dot{\alpha} + ... \\ + \frac{L}{2} g m_b \cos(\alpha) + g m_B r \cos(\alpha) = \tau_b \end{bmatrix} \tag{4}$$

$$\left(m_B + \frac{J_B}{R_B}\right)\ddot{r} - m_B r\dot{\alpha}^2 + m_B g \sin(\alpha) = 0 \tag{5}$$

The transformation of torque into voltage:

$$\tau_i = \frac{K_t}{K_m} u - \frac{K_t}{K_m} K_b \omega \tag{6}$$

By converting the input into voltage, the system's differential equation is expressed as:

$$\begin{cases} \ddot{\alpha} = \dfrac{\left[\begin{array}{l}-(2T_f K_z - 2uK_x K_z + 2\dot{\alpha}K_y K_z{}^2 \\ +4\dot{\alpha}m_B r\dot{r} + Lgm_b\cos\alpha + 2gm_B r\cos\alpha + 2C_m\dot{\alpha}K_z{}^2)\end{array}\right]}{2(m_B r^2 + J_b + J_m K_z{}^2)} \\ \ddot{r} = \dfrac{-(R^2(-m_B r\dot{\alpha}^2 + gm_B\sin\alpha))}{(m_B R^2 + J_B)} \end{cases} \tag{7}$$

Based on Equations (7), the state-space equations of the system are established as follows:

$$\begin{cases} \dot{x}_1 = x_2 \\ \dot{x}_2 = f_1(x) + g_1(x).u \\ \dot{x}_3 = x_4 \\ \dot{x}_4 = f_2(x) + g_2(x).u \end{cases}$$

where:

$$x = \begin{bmatrix} x_1 & x_2 & x_3 & x_4 \end{bmatrix}^T = \begin{bmatrix} r & \dot{r} & \alpha & \dot{\alpha} \end{bmatrix}^T$$

$$f_1 = \frac{-(R^2(-m_B r\dot{\alpha}^2 + gm_B\sin\alpha))}{(m_B R^2 + J_B)}$$

$$f_2 = \frac{\left[\begin{array}{l}-(2T_f K_3 + 2\dot{\alpha}K_2 K_3{}^2 \\ +4\dot{\alpha}m_B r\dot{r} + Lgm_b\cos\alpha + 2gm_B r\cos\alpha + 2C_m\dot{\alpha}K_3{}^2)\end{array}\right]}{2(m_B r^2 + J_b + J_m K_3 K^2)}$$

$$g_2 = \frac{(2K_1 K_3)}{2(m_B r^2 + J_b + J_m K_3{}^2)}$$

3. Proposed LQR-Backstepping Controller

To obtain a linear mathematical model, the nonlinear system is linearized around its operating point. Consider an *n*-th order nonlinear system featuring p inputs and q outputs, governed by the state equation:

$$\begin{cases} \dot{x}(t) = f(x(t), u(t)) \\ y(t) = h(x(t), u(t)) \end{cases} \tag{8}$$

where: $\dot{x}(t)$ is the state vector; $u(t)$ is the input signal vector; $y(t)$ is the output signal vector; $f(x,u)$ is the vector function describing the dynamic characteristics of the nonlinear system.

By expanding the governing dynamic equation about an arbitrary point using a Taylor series, we obtain:

$$\begin{aligned} f(x,u) \approx f(\bar{x},\bar{u}) + \frac{\partial f(x,u)}{\partial x}\Big|_{x=\bar{x},u=\bar{u}}.(x-\bar{x}) \\ + \frac{\partial f(x,u)}{\partial u}\Big|_{x=\bar{x},u=\bar{u}}(u-\bar{u}) \end{aligned} \tag{9}$$

Assuming (8), linearizing the system about the equilibrium point (9) results in the linear state-space representation:

$$\begin{cases} \dot{\tilde{x}}(t) = A\tilde{x}(t) + B\tilde{u}(t) \\ \tilde{y}(t) = C\tilde{x}(t) + D\tilde{u}(t) \end{cases} \tag{10}$$

The linearized system is generally represented by the following equation:

$$\begin{cases} \dot{x}(t) = Ax(t) + Bu(t) \\ y(t) = Cx(t) \end{cases} \tag{11}$$

The Jacobian matrices, A and B, are computed through partial differentiation:

$$\begin{cases} A = \dfrac{\partial f(x,u)}{\partial x}\Big|_{x=\bar{x},u=\bar{u}} \\ B = \dfrac{\partial f(x,u)}{\partial u}\Big|_{x=\bar{x},u=\bar{u}} \\ C = \dfrac{\partial h(x,u)}{\partial x}\Big|_{x=\bar{x},u=\bar{u}} \end{cases} \tag{12}$$

The proposed control law combines the LQR gain matrix **K** with the system states to generate the control input within a backstepping design framework.

Based on the LQR gain matrix K, the control input is designed as follows:

$$\mathbf{K} = \begin{bmatrix} K_1 & K_2 & K_3 & K_4 \end{bmatrix} \tag{13}$$

The system state vector is defined as follows:

$$x = \begin{bmatrix} r & \dot{r} & \dot{\alpha} \end{bmatrix}^T \tag{14}$$

The first step in the backstepping design is to define the tracking error as follows:

$$z_1 = -K_1 r - K_2\dot{r} - K_3\alpha - K_4\dot{\alpha} \tag{15}$$

The time derivative of the error z_1 variable is computed as follows:

$$\dot{z}_1 = -K_1\dot{r} - K_2\ddot{r} - K_3\dot{\alpha} - K_4\ddot{\alpha} \tag{16}$$

Step 2: The next error variable z_2, is defined as follows:

$$z_2 = \dot{z}_1 + c_1 z_1 \tag{17}$$

$$\begin{aligned} \dot{z}_2 = -K_1(f_1 + g_1 u) - K_2\left(\dot{f}_1 + g_1 u\right) \\ -K_3(f_2 + g_2 u) - K_4\left(\dot{f}_2 + \dot{g}_2 u\right) + \mathrm{c}_1\dot{z}_1 \end{aligned} \tag{18}$$

In this expression, $\dot{z}_1$ involves a third-order derivative, which can be represented as:

$$\frac{d}{dt}(\ddot{r}) = \sum_{x\in\{r,\dot{r},\alpha,\dot{\alpha}\}} \frac{\partial\ddot{r}}{\partial x}\dot{x} \tag{19}$$

In which $\ddot{r} = f(r,\dot{r},\alpha,\dot{\alpha})$

$$\begin{cases} \ddot{r} = \dot{f}_1 + \dot{g}_1 u \\ \ddot{\alpha} = \dot{f}_2 + \dot{g}_2 u \end{cases} \tag{20}$$

$$\begin{aligned} \dot{f}_1 = \frac{RB^2\dot{\alpha}^2 m_B\dot{r}}{m_B RB^2 + J_B} - \frac{R_B{}^2\dot{a}gm_B cos(a)}{mB * RB^2 + JB} \\ \frac{2R_B{}^2\dot{a}m_B r(T_f k_3 + C_m\dot{a}k_3{}^2 + \dot{a}k_2 k_3{}^2 + 2\dot{a}m_B r\dot{r}}{(m_B R_B{}^2 + J_B)(J_m k_3{}^2 + m_B r^2 + J_b)} \\ -\frac{+0.5Lgm_L cos(a) + gmBrcos(a))}{(m_B R_B{}^2 + J_B)(J_m k_3{}^2 + m_B r^2 + J_b)} \end{aligned} \tag{21}$$

$$\dot{f}_2 = \frac{\dot{a}\left(0.5Lgm_b sin(a) + gm_{\mathbf{B}} r sin(a)\right)}{J_m k_3^{\ 2} + m_B r^2 + J_b}$$
$$- \frac{\dot{r}((2\dot{a}m_B\dot{r} + gm_B cos(a)}{J_m k_3^{\ 2} + m_B r^2 + J_b}$$
$$- \frac{(2m_B r(T_f k_3 + C_m \dot{a} k_3^{\ 2} + \dot{a} k_2 k_3^{\ 2} + 2\dot{a}m_B r\dot{r} + 0.5Lgm_b cos(a) + gm_B r cos(a))}{(J_m k_3^{\ 2} + m_B r^2 + J_b)^2}$$
$$+ \frac{(C_m k_3^{\ 2} + k_2 k_3^{\ 2} + 2m_B r\dot{r})(T_f k_3 + C_m \dot{a} k_3^{\ 2} + \dot{a} k_2 k_3^{\ 2} + 2\dot{a}m_B r\dot{r} + 0.5Lgm_b cos(a) + gm_B r cos(a))}{(J_m k_3^{\ 2} + m_B r^2 + J_b)^2}$$
$$+ \frac{(2R_B^{\ 2}\dot{a}m_B r(-m_B r\dot{a}^2 + gm_B sin(a)))}{(m_B R_B^{\ 2} + J_B)(J_m k_3^{\ 2} + m_B r^2 + J_b)} \quad (22)$$

$$\dot{g}_1 = \frac{2R_B^{\ 2} a k_1 k_3 m_B r}{(m_B R_B^{\ 2} \quad J_B)(J_m k_3^{\ 2} \quad m_B r^2 \quad J_b)} \quad (23)$$

$$\dot{g}_2 = \frac{-(k_1 k_3 * (C_m k_3^{\ 2} \quad k_2 k_3^{\ 2} \quad 4m_B r\dot{r}))}{(J_m k_3^{\ 2} \quad m_B r^2 \quad J_b)^2} \quad (24)$$

Step 3: To ensure asymptotic stability of the tracking errors, we propose a Lyapunov candidate function V_2 incorporating both z_1 and z_2. The construction of V_2 aims to satisfy the stability criterion $\dot{V}_2 < 0$, expressed as:

$$V_2 = \frac{1}{2}z_1^2 \quad \frac{1}{2}z_2^2 \quad (25)$$

Recalling the error dynamics of the first stage, we have:

$$\dot{z}_1 = z_2 - c_1 z_1 \quad (26)$$

The time derivative of V_2 along the system trajectories is computed as:

$$\dot{V}_2 = z_1\dot{z}_1 \quad z_2\dot{z}_2 \quad (27)$$

Substituting (26) into (27) yields the expanded form of the Lyapunov derivative:

$$\dot{V}_2 = z_1(z_2 - c_1 z_1) \quad z_2\dot{z}_2 = -c_1 z_1^{\ 2} \quad z_2(z_1 \quad \dot{z}_2) \quad (28)$$

To ensure that $\dot{V}_2$ is negative definite, the virtual control law and the second error dynamics are designed such that:

$$\dot{z}_2 = -z_1 - c_2 z_2 \quad (29)$$

Under this choice, the Lyapunov derivative simplifies to a negative semi-definite form, guaranteeing the non-increase of the energy function:

$$\dot{V}_2 = -c_1 z_1^{\ 2} - c_2 z_2^{\ 2} \quad (30)$$

By substituting the system dynamics into (29), the actual control input *u* is explicitly derived as:

$$u = \frac{-z_1 - c_2 z_2 - c_1\dot{z}_1 + K_1 f_1 + K_2 f_1 + K_3 f_2 + K_4 f_2}{K_1 g_1 \quad K_2 g_1 \quad K_3 g_2 \quad K_4 g_2} \quad (31)$$

$$\ddot{V}_2 = -2c_1\dot{z}_1 z_1 - 2c_2\dot{z}_2 z_2 \quad (32)$$

Since $z_1, z_2, \dot{z}_1, \dot{z}_2$ are bounded, $\ddot{V}_2$ are also bounded. Barbalat's theorem can be applied to prove that both z_1, z_2 converge to 0 as $t \to \infty$.

$$\ddot{V}_2 = -2c_1\dot{z}_1 z_1 - 2c_2\dot{z}_2 z_2 \quad (33)$$

4. Simulation Results

The simulation is conducted for 100 s with a fixed sampling period of 0.01 s [16]. To ensure high fidelity between the numerical model and experimental conditions, the sampling rates are perfectly synchronized. Consequently, each simulation trial yields a total of $N = 10{,}001$ data points. The control parameters are optimized using the Particle Swarm Optimization (PSO) algorithm, with the fitness function based on the system's error performance over a 100-second interval. To handle potential divergence, a safety mechanism is implemented: any parameter set that induces instability is automatically terminated and excluded from the fitness evaluation. Furthermore, the initial state variables are established as $x_{init} = [0.54, 0, -0.1319, 0]^T$ (with x_3 in radians). The entire control framework is developed and validated within the MATLAB/Simulink environment

In this study, simulations are conducted in two cases:

Case 1: The simulation is conducted to evaluate the controller's ability to stabilize the ball at a fixed position on the beam under ideal conditions.

Case 2: The simulation is designed to assess the controller's performance in tracking a time-varying (sinusoidal) reference under dynamic conditions.

Tab. 2 Parameters of the LQR-BSP combined controller:

Nr.	1	2
Parameter	c_1	c_2
Value	220	20

The ball is stabilized at a specific position.

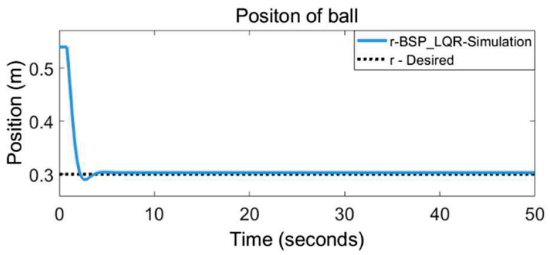


Fig. 2. Simulation Results of Ball Position (m) BSP_LQR in case 1

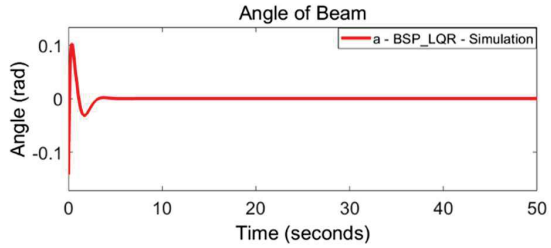


Fig. 3. Simulation Results of Beam Deflection Angle (rad) BSP_LQR in case 1

The simulation results in Figs. 1 and 2 demonstrate that the BSP–LQR controller effectively stabilizes the ball-and-beam system around the desired equilibrium position.

Specifically, in Fig. 1, the ball position response $r$shows a small initial overshoot due to the initial conditions, after which it quickly converges to the desired reference and remains stable with nearly zero steady-state error. The measured trajectory closely follows the reference signal, indicating high tracking accuracy and good control performance.

In Fig. 2, the beam angle shows a brief transient oscillation at the start with a relatively small amplitude, which is rapidly damped. The angle then converges to approximately 0 rad and remains stable over time, confirming that the system maintains its equilibrium without sustained oscillations.

These results indicate that the BSP–LQR controller achieves both precise ball position regulation and stable beam angle control. The fast response, low overshoot, and absence of persistent oscillations highlight the effectiveness of the proposed control approach for the ball-and-beam system.

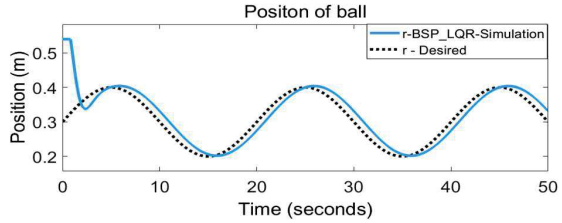


Fig. 4. Simulation Results of Ball Position (m) BSP_LQR in case 2

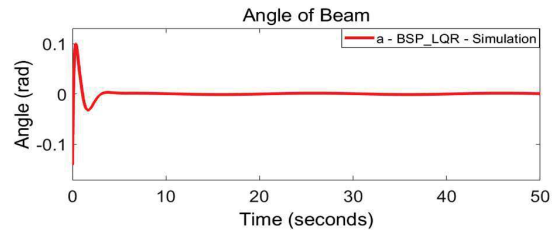


Fig. 5. Simulation Results of Beam Deflection Angle (rad) BSP_LQR in case 2

The simulation results shown in Fig. 3 and Fig. 4 further confirm the effectiveness of the BSP–LQR controller in trajectory tracking for the ball-and-beam.

In Fig. 3, the ball position $r$successfully follows the sinusoidal reference trajectory. The output signal closely matches the desired curve, with only a small phase lag and a minor amplitude deviation. This indicates that the controller achieves good tracking performance even for time-varying references. Response is smooth and stable, without excessive oscillations or distortion, demonstrating the controller's ability to handle continuous dynamic changes.

In Fig. 4, the beam angle exhibits a brief transient at the initial stage, followed by rapid convergence to zero. During steady-state operation, the angle remains very close to 0 rad, with negligible fluctuations, ensuring the beam stays nearly horizontal and enabling the ball to track the desired trajectory.

These results show that the BSP–LQR controller not only stabilizes the system but also provides accurate and smooth trajectory tracking. The small tracking error, fast transient response, and stable beam behavior highlight the robustness and effectiveness of the proposed control strategy for dynamic reference inputs.

5. Conclusions

This study has investigated the control performance of the BSP–LQR controller for the ball-and-beam system under two typical scenarios: stabilization at a fixed position and tracking of a time-varying (sinusoidal) reference.

In the first case, where the objective is to regulate the ball to a constant position, the simulation results demonstrate that the controller achieves fast convergence with minimal overshoot and nearly zero steady-state error. The beam angle quickly stabilizes near zero after a short transient phase, ensuring the system remains in equilibrium without sustained oscillations. This confirms the effectiveness of the BSP–LQR approach in stabilizing an inherently unstable system.

In the second case, involving sinusoidal trajectory tracking, the controller successfully enables the ball to follow the desired reference with high accuracy. Although a slight phase lag and small amplitude deviation are observed, the overall tracking performance remains smooth and stable. Meanwhile, the beam angle remains well-regulated around zero, indicating that the controller can handle dynamic reference changes without compromising system stability.

The results from both cases highlight that the BSP–LQR controller provides a reliable and efficient solution for the ball-and-beam system. It not only ensures stable regulation but also achieves accurate trajectory tracking, demonstrating robustness and adaptability under different operating conditions.

Acknowledgement

This research was funded by Ho Chi Minh City University of Technology and Engineering, Vietnam, under grant No. SV2026- 440. We want to give thanks to PhD. Van-Dong-Hai Nguyen (HCM-UTE) due to his

supervision for this research. We, authors, are grateful for these supports.

6. References

[1] Nguyen D.-A.-Q., et al.: "Application of LQG Control for Pendubot System", Journal of Fuzzy Systems and Control, Vol. 2, No. 1, pp. 40–44, 2024.
[2] Nguyen D.-A.-Q., et al.: "Adaptive Evaluation of LQR Control using Particle Swarm Optimization for Pendubot", Journal of Fuzzy Systems and Control, Vol. 2, No. 2, pp. 58–66, 2024.
[3] Nguyen Q.-T., et al.: "Load Variation Estimation and Hierarchical Sliding Mode Control for Pendubot Using Swarm Algorithm", Robotica & Management, Vol. 30, No. 1, pp. 32–37, 2025.
[4] Nguyen Q.-T., et al.: "Sliding Mode Control for Ball in Tube", Robotica & Management, Vol. 30, No. 1, pp. 12–17, 2025.
[5] Rudra S., Barai R. K., Maitra M.: "Block Backstepping Control of the Underactuated Mechanical Systems", Springer, Singapore, 2017.
[6] Nguyen Q.-T., et al.: "Real-Time Trajectory Tracking Control of a DC Motor Using a Self-Tuning Regulator with Online Parameter Estimation", Control Systems and Optimization Letters, Vol. 4, No. 1, 2026.
[7] Ali M., Mandal S.: "Kalman Filter Based Control of Inverted Pendulum System", IFAC-PapersOnLine, Vol. 55, No. 1, pp. 58–63, 2022.
[8] Bajodah A. H., Ansari U.: "Rotary Inverted Pendulum Control using Robust Generalized Dynamic Inversion with Adaptive Neural Estimation", IFAC-PapersOnLine, Vol. 56, No. 2, pp. 10570–10575, 2023.
[9] Bezci Y. E., et al.: "Classical and intelligent methods in model extraction and stabilization of a dual-axis reaction wheel pendulum: A comparative study", Results in Engineering, Vol. 16, p. 100685, 2022.
[10] Chacko S. J., C N. P., Abraham R. J.: "Optimizing LQR controllers: A comparative study", Results in Control and Optimization, Vol. 14, p. 100387, 2024.
[11] Kharola A., Patil P., Raiwani S., Rajput D.: "A comparison study for control and stabilisation of inverted pendulum on inclined surface (IPIS) using PID and fuzzy controllers", Perspectives in Science, Vol. 8, pp. 187–190, 2016.
[12] Qu Y., Liu Z., Cai L.: "Simultaneous planning and executing (SPAE) control for a fourth-order underactuated inverted pendulum with double-layer asynchronous convergence", ISA Transactions, Vol. 163, pp. 162–171, 2025.
[13] Kumar E. V., Jerome J.: "Robust LQR Controller Design for Stabilizing and Trajectory Tracking of Inverted Pendulum", Procedia Engineering, Vol. 64, pp. 169–178, 2013.
[14] Wang J.-J.: "Simulation studies of inverted pendulum based on PID controllers", Simulation Modelling Practice and Theory, Vol. 19, No. 1, pp. 440–449, 2011.
[15] Zhu Q., Lei C., Shi B., Zhang J., Wang J.: "Model-free robust underactuated control of inverted pendulums", Journal of the Franklin Institute, Vol. 362, No. 13, p. 107911, 2025.
[16] Tran V. H. L., Le T. H.: "Trajectory Tracking Control For An Offset Axis Ball And Beam System", Graduation Thesis, Ho Chi Minh City University of Technology and Education, Ho Chi Minh City, 2025.
[17] Maalini P. M., Prabhakar G., Selvaperumal S.: "Modelling and control of ball and beam system using PID controller", 2016 International Conference on Advanced Communication Control and Computing Technologies (ICACCCT), pp. 322-326, 2016.
[18] Keshmiri M., Jahromi A. F., Mohebbi A., Amoozgar M. H., Xie W.-F.: "Modeling and control of ball and beam system using model based and non-model based control approaches", International Journal on smart sensing and intelligent systems, Vol. 5, No. 1, pp. 14-35, 2012.
[19] Schoukens J., Ljung L.: "Nonlinear system identification: A user-oriented road map", IEEE Control Systems Magazine, Vol. 39, No. 6, pp. 28-99, 2019.
[20] Brunton S. L., Proctor J. L., Kutz J. N.: "Discovering governing equations from data by sparse identification of nonlinear dynamical systems", Proceedings of the national academy of sciences, Vol. 113, No. 15, pp. 3932-3937, 2016.